JOURNAL OF MATERIALS SCIENCE 27 (1992) 4373–4380

# Creep behaviour of a heat-resistant ferritic chromium steel in terms of stress exponents

F. GROISBÖCK
*Institut für Metallkunde und Werkstoffprüfung, Montanuniversität Leoben, A-8700 Leoben, Austria*

In many publications the high-temperature deformation behaviour of materials is described by the stress sensitivity of steady-state creep rate, the creep exponent, $n$. In order to investigate the mechanisms of dislocation motion, it is more promising to evaluate the constant structure creep properties. This leads to the constant structure creep exponent, $m'$, which is not influenced by the stress dependence of the substructure. Therefore, the investigation of deformation mechanisms is less difficult. Additionally, $m'$ is the basis for the calculation of the effective stress exponent, $m$, of dislocation velocity, which permits the investigation of the strength of interactions between alloying atoms and moving dislocations. It is shown that the creep exponent, $n$, is between 5 and 10 in the power-law creep region (where diffusion-controlled glide processes of dislocations cause deformation). However, it increases to about 50, if exponential creep is working (in this region the glide processes are thermally activated but diffusion is not the rate-controlling mechanism). The constant structure creep exponent, $m'$, is relatively small and independent of stress in the power-law creep region. It increases almost linearly with the applied stress, if thermally activated glide dominates creep. The evaluation of the stress exponent, $m$, which can be calculated from $m'$ and the effective stresses, showed that dislocation motion is influenced by alloying atoms as long as power-law creep works. There is experimental evidence that power-law breakdown is due to a breakdown of the alloying effect, because dislocations can escape from their dragging Cottrell clouds at high applied stresses.

## 1. Introduction

Ferritic chromium steels have worse creep properties than austenitic steels. This is a consequence of faster diffusion processes. There are, however, two reasons for their application in modern high-temperature equipment: first, their advantageous high-temperature corrosion properties, especially in case of sulphur-containing environments, and second their lower price due to the absence of nickel. High-temperature application of ferritic chromium steels is usually restricted to conditions with very low stresses. In order to improve their application, it is necessary to investigate creep mechanisms and furnish creep data.

Time-dependent deformation usually takes place when more than 40–50% of the melting temperature is reached. Depending on the deformation mechanism working, the correlation between strain rate, $\dot{\varepsilon}$, and applied stress, $\sigma$, is

$$\dot{\varepsilon} = A(T)\left(\frac{\sigma}{G}\right)^n \quad (1)$$

which indicates power-law creep, or

$$\dot{\varepsilon} = B(T)\exp(\beta\sigma) \quad (2)$$

which is called exponential creep or power-law breakdown [1, 2]. $A(T)$ and $B(T)$ are terms depending on the temperature $T$. $G$ is the shear modulus, which is slightly temperature dependent. As the substructure developing during deformation depends on various influences, e.g. the applied stress, deformation temperature and the type of material, the creep exponent, $n$, can take a wide range of values. In the case of single-phase alloys with a strong influence of alloying atoms, as for example Al–Mg alloys (alloy-type creep), $n$ takes values of about 3. It rises to about 5–10 in the case of pure metals, or alloys which behave like pure metals (metal-type creep) [3]. Sometimes very high values of $n$ (up to 40 [2]) are reported. Except in the case of particle-hardened alloys such as the modern nickel-based materials, where high $n$ values are caused by interaction between dislocations and particles [4]; this indicates that the creep mechanism working is exponential creep [2].

Metal-type power-law creep is assumed to be dominated by dislocation climb processes. The most important feature of the substructure is the highly ordered dislocation networks of subgrain walls. These networks are sites of high local dislocation densities and therefore of high local stresses [5]. The dislocation density inside the subgrains is low [6]. Long-range internal stresses, which arise because of the inhomogeneous distribution of dislocations, oppose

0022–2461  

dislocation motion in the subgrain interior. As the magnitude of interaction between dislocations and foreign atoms increases, the tendency to build regular dislocation networks decreases. High interaction forces lead to a relatively homogeneous dislocation distribution. Slow drag-controlled glide of dislocations is now the rate-controlling process [7].

Many alloys do not show any influence of foreign atoms on the steady state creep properties such as the creep exponent, $n$ [3]. However, there are more sensitive methods to check whether there is an alloying effect or not. One of them is the determination of the constant structure creep properties [8]. In combination with measurements of internal stresses (from transient dip tests) it is possible to determine the exponent $m$, which relates the velocity, $v$, of a moving dislocation to the effective stress, $\sigma_e$, acting on it [8]

$$v \sim \sigma_e^m \tag{3}$$

If $m$ values near unity are observed, the dislocation motion is drag controlled [8, 9], although no influence on the steady state creep behaviour can be found [10]. If $m$ deviates largely from unity, dislocation motion becomes jerky and glide is no longer drag controlled.

In this paper the steady state and the constant structure creep properties of a ferritic chromium steel are presented. The steady state strain-rate data are plotted in the usual way as a function of applied stress in a double-logarithmic diagram. The resulting creep exponents are interpreted in terms of different deformation mechanisms. Stress relaxation data are used to describe the constant structure creep properties. In combination with some previously published data on internal stresses, the stress exponent, $m$, of dislocation motion is calculated. The results are discussed in terms of creep mechanisms working and the influence of alloying atoms.

## 2. Experimental procedure

A heat-resistant ferritic chromium steel (chemical composition: 0.1% C, ≈18% Cr, ≈1% Si and ≈1% Al; Fe remainder) was tested in two structural conditions. The coarser material had a grain size of about 50 μm and large carbides (up to 20 μm), while the finer material showed grains about 10 μm in size and small carbides (0.1–1 μm). For a more detailed description of the material investigated, as well as the test procedures for the determination of stationary creep properties and internal stresses, see [11].

Stress relaxation tests were performed at temperatures between 500 and 750 °C at initial strain rates, $\dot{\varepsilon}_0$, of about $5 \times 10^{-7}$–$5 \times 10^{-3}$ $s^{-1}$. Relaxation tests were carried out when the steady state deformation rate was reached. When those deformation conditions did not lead to a steady state (in the exponential creep region), stress relaxation was started close to the largest deformation resistance (i.e. the minimum creep rate in a constant stress creep test). Two testing facilities were used. With an Instron-type machine, relaxation was started by stopping crosshead motion. With a mechanical constant stress testing device, which is described in detail in [12], relaxation was started when a mechanical stop was reached by the loading system. The latter testing facility has some advantages in the case of higher initial strain rates because it is less rigid. This leads to a flatter stress–time curve which can be better evaluated. On the other hand, the relatively rigid Instron-type testing machine avoids very flat stress–relaxation curves in the case of small initial strain rates. There was no difference between the results yielded by the two testing facilities.

The strain rate, $\dot{\varepsilon}_r$, during the relaxation test can be calculated from the rate of stress decrease, $\dot{\sigma} = d\sigma/dt$

$$\dot{\varepsilon}_r = \frac{-\dot{\sigma}}{E^*} \tag{4}$$

where $E^*$ is a modulus of elasticity, which combines the stiffness of the testing machine and the Young's modulus of the specimen [2] ($1/E^* = 1/E + A_0/l_0R$). $E$ is the elastic modulus of the investigated material at the test temperature ($E \approx 80$ GPa [12]), $A_0$ is the cross-section of the deformed specimen, $l_0$ is the length of the deformed specimen and $R$ is the stiffness of the testing machine. For the determination of the effective stress exponent, $m$, of dislocation motion the mechanically (with transient dip tests) measured $\sigma_i$ data were used.

## 3. Results

### 3.1. Results of steady state creep testing

Fig. 1a shows the stress dependence of the strain rate for all test conditions in a double-logarithmic diagram. It can be seen that all different groups of data points show a change in the stress dependence of the strain rate, $\dot{\varepsilon}$. This indicates a transition in creep mechanisms. At low stresses or low strain rates (power-law creep is operating) the creep exponent, $n$, is in the range 5–10. This quantity increases in the high stress–high strain rate region where exponential creep dominates to at least 8 and up to more than 50. From a mathematical point of view use of Equation 1 is not allowed and therefore neither is a double-logarithmic diagram of strain rate and stress in the exponential creep region, but for practical reasons this is done to show that there is a change in material behaviour.

Fig. 1b shows the creep exponents, $n$, which are evaluated for each temperature and each material below and beyond the transition in creep mechanisms. It can be seen that the creep exponent, $n$, of the power law increases only slightly with decreasing temperature. Except for the value at 600 °C of the coarser (conventional) material, there is no big difference between the two investigated material states in the case of power-law creep. The same conclusion can be drawn for the exponential values. Owing to the fact that a very small range of strain rate has been investigated in the exponential creep region, the difference between creep exponents of power law and exponential creep is low at high temperatures. In the vicinity of transition, the stress dependence of the strain rate in the exponential creep region is smaller than it is far away. Another reason for relatively low creep exponents at high temperatures (not only in the

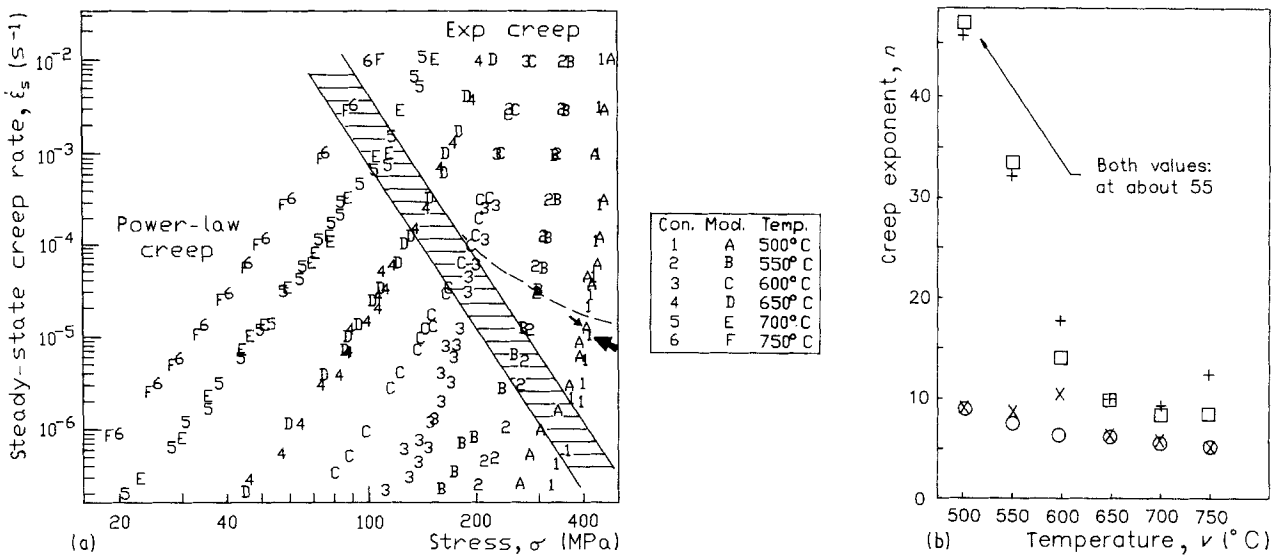


*Figure 1* Steady-state creep properties of the investigated heat-resistant ferritic steel. (a) Double-logarithmic plot of steady-state creep rate and applied stress. Hatched area: the transition between power law and exponential creep (conventional material). (– – –) The shift of this transition for the modified material. (b) Creep exponent, $n$, in the region of (○, ×) power-law and (□, +) exponential creep for (○, □) modified and (×, +) conventional materials.

exponential creep region) is the fast diffusion, which leads to more regular structures, e.g. to well-knitted subgrain boundaries in the power-law region. As a result the creep behaviour comes closer to the creep theories which describe the deformation behaviour in the case of a well-developed substructure [5].

The creep exponent, $n$, of the power-law creep mechanism takes values near 5 (700–750 °C) to 10 (500–550 °C). Following Sherby and Burke [3], this may be interpreted in terms of very soft interactions between dislocations and foreign atoms. This would mean that metal-type power-law creep is working in the case of the investigated ferritic chromium steel. The following investigation shows that this conclusion is misleading.

## 3.2. Constant structure creep exponent

From a series of normal creep tests (at a fixed temperature) the stress dependence of the (steady state) creep rate, the stress exponent, $n$, can be evaluated. This quantity is influenced by the substructure developing during the creep test, which depends on the applied stress (e.g. the subgrain size decreases with increasing stress [6]). Normally it is not possible to distinguish between the influences of substructural and stress changes on the resulting strain rate. The constant structure creep exponent, $m'$, which offers a large potential for the investigation of creep mechanisms and permits identification of the nature of dislocation motion, can be determined by means of stress dip tests [8] or stress relaxation tests [8, 12]. The latter possibility was used for this paper.

After a specimen was crept to a certain amount of deformation, the relaxation test was started with an initial stress, $\sigma_0$, and an initial strain rate, $\dot{\varepsilon}_0$. Forward deformation continues because of a positive effective stress as is observed when small stress reductions are applied in dip tests [8, 11]. The inelastic strain of forward creep has to be compensated by an elastic deformation of the specimen and the loaded parts of the testing machine because after the start of relaxation no overall deformation is permitted by the testing facility [2]. The reduction in stored elastic deformation causes the stress to decrease.

With Equation 4 the strain rate during the stress relaxation test can be calculated easily. The constant stress creep exponent is then given by

$$m' = \mathrm{d}\ln(\dot{\varepsilon}_r/\dot{\varepsilon}_0)/\mathrm{d}\ln(\sigma_r/\sigma_0) \qquad (5)$$

$\dot{\varepsilon}_r$ is the calculated strain rate at a stress $\sigma_r$, $\dot{\varepsilon}_0$ and $\sigma_0$ are strain rate and stress, respectively, before starting relaxation. For practical reasons it is better to calculate $\dot{\varepsilon}_0$ in the same way as $\dot{\varepsilon}_r$, i.e. from the rate of stress decrease, $\dot{\sigma}_0$, at the moment of relaxation start. In this manner errors arising from the determination of $E^*$ can be avoided, which can be easily seen by combining Equations 4 and 5. The same result can be obtained if $m'$ is evaluated directly from the rates of stress decrease, $m' = \mathrm{d}\log(\dot{\sigma}_r/\dot{\sigma}_0)/\mathrm{d}\log(\sigma_r/\sigma_0)$ and therefore with the help of a diagram, $\log(\dot{\sigma}_r/\dot{\sigma}_0)$ over $\log(\sigma_r/\sigma_0)$. As the latter method leads to problems when comparing the results of stress relaxation tests with the steady state deformation behaviour, it was not used here.

Fig. 2a shows the results of three relaxation tests at different starting stresses in the region of power-law creep, while Fig. 2b shows three relaxation curves in the exponential creep region (note the different scale of the stress axis). For comparison, the results of a hypothetic stress relaxation test are shown, which are derived when the material behaves as in steady-state deformation (dotted lines). The slope of these lines is given by the steady-state creep exponent, $n$.

In all relaxation tests at 700 °C within the power-law creep region, the constant structure creep exponent, $m'$, was found to be near 8.5 (Fig. 2a), while the steady-state creep exponent, $n$, was approximately 5. With increasing relaxation time the relaxation curves

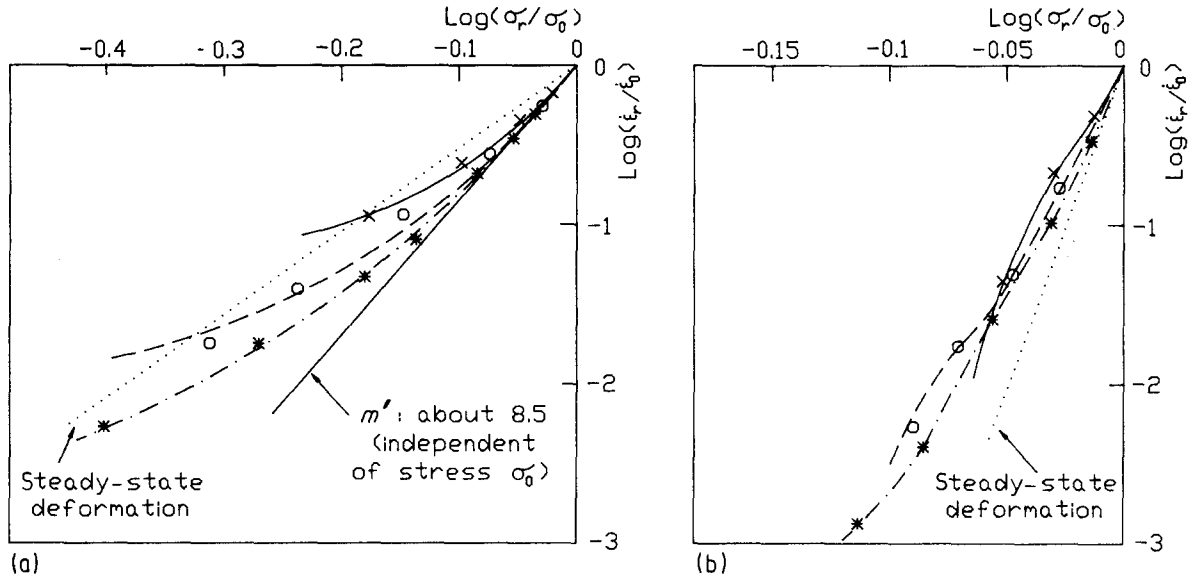


*Figure 2* Evaluation of stress relaxation tests with the aim of determining the constant structure creep exponent, $m'$. (a) Typical relaxation curves at 700 °C (power-law creep); $\sigma_0$ (MPa): (*) 106, (○) 72, (×) 38. (b) Typical relaxation curves at 500 °C (exponential creep); $\sigma_0$ (MPa): (*) 436, (●) 394, (×) 366. $m'$ for $\sigma_r \rightarrow \sigma_0$: (*) 32, (○) 30, (×) 25.5.

become flatter, which means that the stress dependence of the relaxation rate decreases continuously. All relaxation tests at 700 °C cut through the steady-state line. The point of intersection depends on the starting stress. At high starting stresses the relative decrease for the intersection is higher than at lower starting stresses.

When exponential creep is working, the stress dependence of the relaxation rate is smaller than it would be under steady-state conditions ($m'$ is smaller than $n$). $m'$ depends on the starting stress and increases from 25.5 at $\sigma_0 = 366$ MPa up to 32 at $\sigma_0 = 436$ MPa, while the steady-state creep exponent, $n$, is larger than 50 (Fig. 1b). Two relaxation curves ($\sigma_0 = 366$ and 394 MPa) are S-shaped, showing a decrease in steepness after the beginning of relaxation and afterwards an increase, which is due to ceasing deformation at long relaxation times (about 1 h). The relaxation curve started at 436 MPa will be S-shaped too, but the increase in steepness after the transition point lies outside the diagram.

Fig. 3 shows data of the constant structure creep exponent, $m'$, derived at various temperatures over a wide range of applied stresses. All $m'$ values of the power-law creep region (approximately the left-hand third of stress range in Fig. 3) lie between 7.5 and 9.5 without showing a stress dependence. Additionally, it can be seen that $m'$ is almost always larger than the stress-dependent exponent, $n$. In the exponential creep region the exponent $m'$ increases nearly linearly with applied stress (the results obtained in the region of exponential creep are marked with arrows). There is a small difference between the two investigated material states: $m'$ values of the conventional material are always larger than those of the modified alloy at the same applied stress. As mentioned above, the constant structure creep exponent is smaller than the steady state creep exponent.

### 3.3. Effective stress exponent of dislocation velocity, $m$

The exponent, $m$, of dislocation motion (Equation 3) can be calculated from the constant structure creep exponent, $m'$, and the mean effective stress, $\sigma_e$ [8]

$$m = m' \frac{\sigma_e}{\sigma} \tag{7}$$

The effective and internal stresses are measured by means of stress transient dip tests using an extrapolation method to exclude the influence of recovery during the dip operation [11]. The results of internal stress measurements are presented in Reference 11. To obtain highly accurate results for the exponent $m$, it is necessary to take only $\sigma_e$ values, which are determined by mechanical (dip-) tests. $\sigma_e$-values evaluated from dislocation bowing are quantitatively too uncertain.

The effective stress exponent, $m$, can be determined only at a temperature of 600 °C [11] because dip tests were carried out only at this temperature. Fig. 4 shows evaluated results for both materials. The transition between power-law and exponential creep is marked with a hatched area involving the slightly different values for both material states. $m$ is about 1 in the power-law region but, with transition to exponential creep, increases to values of 4–5. There may be a step in $m$ at the transition of the deformation mechanism, as is indicated for the conventional material. The results for the modified material show a more continuous increase of $m$.

Generally it can be said that the effective stress exponent, $m$, takes values near unity in the power-law creep region. Small deviations are not substantial, because determination of $m$ is influenced by errors in $m'$ and $\sigma_e$: both may reach 20% or even more of the true value. The increase in $m$ in the exponential creep region is too large to be a result of experimental errors. Therefore, it is concluded that there is a substantial

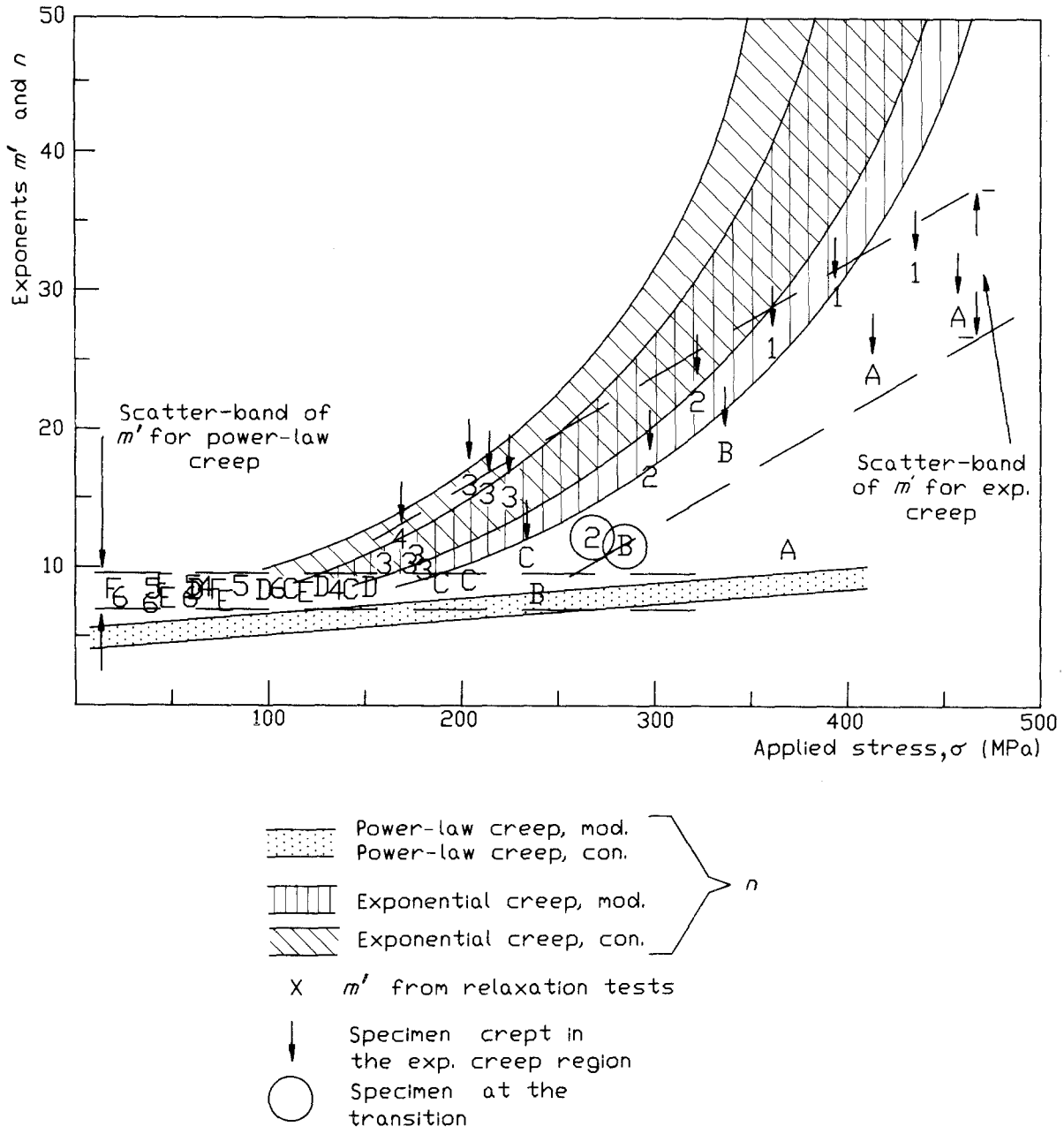


*Figure 3* Constant structure creep exponent, $m'$, as a function of applied stress, $\sigma$. For key, see Fig. 1a. Hatched areas: the stress dependence of the steady-state creep exponent, $n$ (dotted: power-law creep, both materials; hatched: exponential creep).

difference in dislocation motion between power law and exponential creep.

## 4. Discussion

### 4.1. Transition between power-law and exponential creep

As it was shown previously [12, 13], the transition from diffusion-controlled power-law creep to thermally activated glide (exponential creep; diffusion is not rate controlling) occurs at a distinct ratio between the strain rate, $\dot{\varepsilon}$, and the diffusion coefficient $D$: $\dot{\varepsilon}/D \approx 10^{13}\ \mathrm{m}^{-2}$. This is indicated in Fig. 1a (hatched area). It can be seen that for the conventional material the location of change in the creep exponent from low to high values fits well with the calculated transition. The same is found for the modified material at temperatures above 600 °C. At lower temperatures, however, the transition shifts to higher strain rates (indicated by a dashed line in Fig. 1a). This cannot only be found by changing stress dependence of the strain rate (Fig. 1a) but also by means of transmission electron microscopy (TEM) [13]. It was shown previously that between the dashed line and the hatched area (where different deformation mechanisms are operating), the substructure developing during creep is material dependent. The conventional material shows cell structures and regions of relatively homogeneously distributed dislocations (Fig. 5a) with a dislocation arrangement typical of a high rate of intersection processes and a low recovery rate. This is typical of exponential creep. The deformation condition of the specimen shown in Fig. 5a is marked in Fig. 1a with an arrow. It can be seen that this specimen was deformed right in the region of exponential creep. The substructure of a specimen of modified material deformed at nearly the same strain rate and stress as in Fig. 1a (see small arrow) is shown in Fig. 5b. Now subgrain

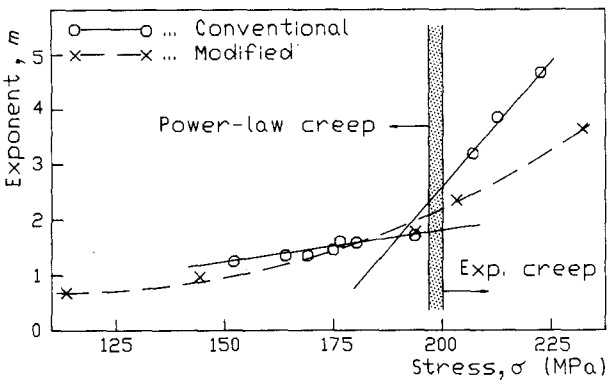


*Figure 4* Effective stress exponent, $m$, of dislocation velocity at 600 °C as a function of stress and material. Hatched area: the transition stress from power-law to exponential creep for (○) conventional and (×) modified materials.

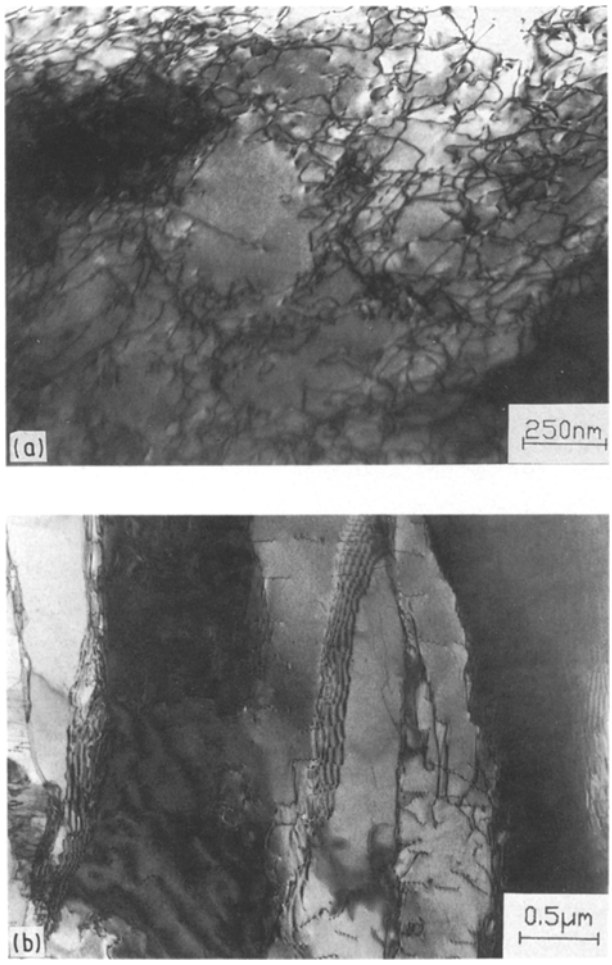


*Figure 5* Transmission electron micrographs of the dislocation arrangement of the two specimens marked in Fig. 1a. (a) Cell structures and regions with homogeneously distributed dislocations dominating in the conventional material (exponential creep, large arrow in Fig. 1a). (b) Subgrain structures with a relatively low dislocation density inside the subgrains are dominating the modified material because power-law creep is working (small arrow in Fig. 1a).

formation is dominating, which is typical of power-law creep. It normally features well-developed subgrain walls with a low dislocation density inside the subgrains and fewer dislocation intersections [12, 13].

The origin of the shift in the transition of strain rate of the modified material is a faster creep rate in the region of power law, see Fig. 1a, temperatures 500–600 °C. As TEM investigations, which were carried out before the specimen was subjected to creep, showed no significant difference in substructure between the modified and the conventional material (e.g. dislocation density and arrangement), it is thought that the acceleration of power-law creep in the modified material at low temperatures is caused by an accelerated diffusion.

The origin of faster diffusion processes may be coarsening processes of carbides, which force diffusion processes in the finer modified material. Another point of interest may be the dissolution of carbon, which was kept in solid solution because the modified material was quenched after the last heat treatment (recrystallization). As carbide precipitation forces chromium diffusion, this would also accelerate diffusion-controlled dislocation motion. Strong evidence for these mechanisms is only found at low temperatures. At higher temperatures the effect of carbide coarsening on the effective diffusion coefficient is smaller, and most of the carbon surplus is precipitated before the specimen reaches steady state. Therefore, the creep behaviour at high temperatures is practically identical for both materials.

## 4.2. Stress exponents

The steady state creep exponent, $n$, of power-law creep increases with falling temperature and increasing stress (Fig. 1b). This is consistent with previously published results, e.g. on pure LiF [14]. Increasing stress sensitivity of the strain rate indicates increasing deviation from the idealized deformation behaviour. This can be seen from internal stress measurements [11] and from the TEM analysis of the substructure, which show increasing irregularity of the dislocation arrangement. The density of dislocations within the subgrains and the number of intersection processes increases with increasing applied stress [12, 13]. This is shown in Fig. 6a and b. Note that Fig. 6b shows a substructure typical of deformation conditions near the vicinity of transition from power law to exponential creep, because there are well-developed subgrain walls (marked with black arrows) and much more irregular cell walls (white arrows). Sometimes, in the vicinity to the transition to exponential creep, the subgrain structure becomes elongated (Fig. 5a).

The relative height of effective stress ($\sigma_e/\sigma$) increases with increasing applied stress because a smaller degree of order of the dislocation arrangement decreases the mean relative height of internal stresses [5, 11]. If the resulting strain rate is thought to be a function of effective stress (Equation 1, $\sigma$ is replaced by $\sigma_e$; note that $A(T)$ changes), it can be seen that the creep exponent decreases to values predicted by creep theories [12, 15].

Compared to the stress-dependent steady state creep exponent, $n$, it seems that the constant structure creep exponent, $m'$, is a quantity more typical of the acting deformation mechanism. The creep exponent,

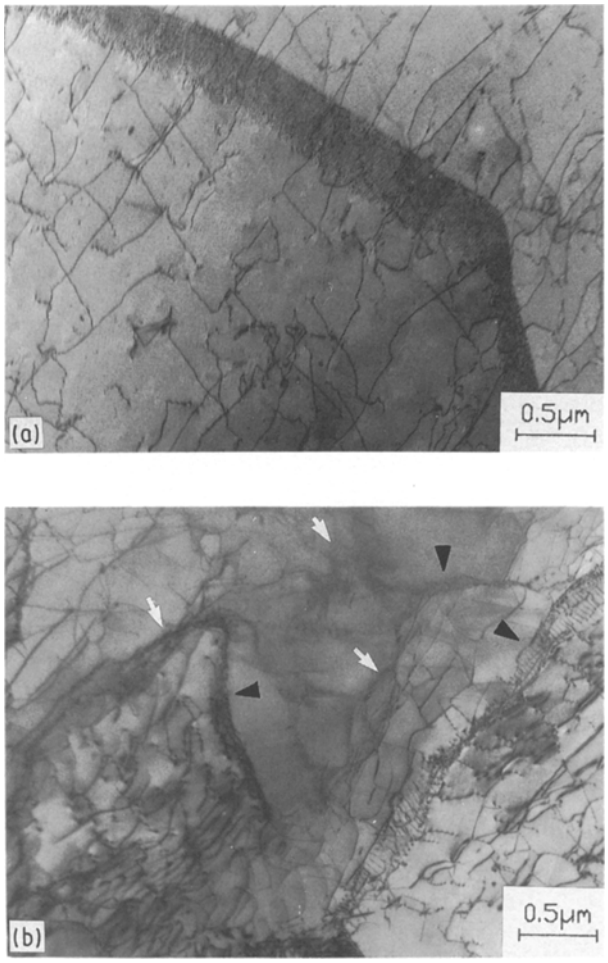


*Figure 6* Substructural changes with increasing applied stress in the power-law region. (a) Substructure of a specimen deformed at about 40 MPa and 700 °C (well in the power-law region). (b) Substructure of a specimen deformed near the transition to exponential creep (at about 180 MPa and 600 °C). Black arrows indicate well-developed subgrain walls, while white arrows indicate less-ordered cell walls.

$m'$, was determined previously by various researchers. Blum *et al.* [10] found $m'$ for an Al–Zn-alloy to be between 7 and 9. In the same temperature and stress range $m'$ rises (stress dependent) to values of about 40 if measurements are made on pure aluminium. This different material behaviour is thought to be a consequence of the influence of zinc atoms. They cause the velocity of moving dislocations to be just slightly altered when the stress is reduced by a small amount. In pure metals, small stress changes lead to large changes in the average dislocation velocity, and therefore a large $m'$ [10].

This can be easily rationalized if we introduce the concept of internal and effective stresses, $\sigma = \sigma_i + \sigma_e$. Pure metals form well-developed subgrain structures [6, 7] with high local stresses in the subgrain walls [5] and relatively high long-range internal stresses in the subgrain interior [5]. Thus, the internal stresses are high and the effective stresses, which force dislocation motion, are low in the case of power-law creep [5, 9]. A small stress reduction has a large influence on the effective stress and thus on the velocity of moving dislocations. As a measureable result, $m'$ is high.

In alloys, even if they are less solution-strengthened than Al–Mg, internal stresses are lower. Therefore the effective stress acting on the dislocations is higher. Small changes in applied stress cause only small changes in the relative height of effective stress. Thus $m'$ is smaller because material reaction to the stress reduction is weaker and not very different from steady-state deformation. In the region of exponential creep (in Fig. 3 all corresponding results are marked with arrows) a nearly linear increase in $m'$ was found for the investigated ferritic steel. The same dependence was found for pure aluminium [10].

A better instrument to clarify whether there is an influence of foreign atoms on the micromechanism of creep is the effective stress exponent of dislocation velocity, $m$. If $m$ takes values near unity (in the region of power-law creep, see Fig. 4), alloying atoms are dragging dislocation motion [9, 16]. This means that the glide step of dislocations between unpinning and reaching the new stable configuration at the next pinning point is controlled by solute atoms (viscous glide of dislocations [16]). Therefore, this type of alloy does not show a "jerky" glide of dislocations after the unpinning process like pure metals do [9]. The overall deformation rate, $\dot{\varepsilon}$, is still controlled by the unpinning process (dislocation climb), which makes the dislocation free to glide. This is the difference compared to the alloy-type creep, as in the case of Al–Mg alloys, where the creep rate is controlled by the viscous glide of dislocations [9].

Results for $m$ indicate that there is no influence of the alloying atoms on dislocation glide in the region of exponential creep. The exponent $m$ is much larger than 1. Therefore, a small increase of effective stress is followed by a large increase of the average dislocation velocity. This is generally attributed to materials without dragging forces between moving dislocations and alloying atoms [9, 16, 17].

### 4.3. Breakdown of alloying effect

When power-law creep is operating, the dislocation glide process is effected by alloying atoms. This leads to a relatively slow dislocation motion. With increasing stress the velocity of mobile dislocations grows and reaches a critical value, where the clouds of foreign atoms cannot follow the moving dislocations. The Cottrell clouds are lost and dislocations become free to glide [16, 17]. This breakdown of the alloying effect leads to a change in the general deformation mechanism from power-law creep to exponential creep, which is accompanied by a change in substructure [13]. A rough estimation of the applied stress, where most of the dislocations are escaping from their dragging clouds, was given by Weertman [16]

$$\sigma \approx 1.8\, G C_{0,i} |\Omega_M - \Omega_i| / \Omega_M \qquad (8)$$

$C_{0,i}$ is the mean molar concentration of the $i$th element, $\Omega_M$ and $\Omega_i$ are the atomic volumes of the matrix and the $i$th atoms, respectively. For the alloying element aluminium ($\Omega_{Al} = 1.66 \times 10^{-23}$ cm$^3$ [18], $\Omega_{Fe} = 1.19 \times 10^{-23}$ cm$^3$ [18], $G \approx 30$ GPa ($G = E/2(1 + \nu)$; $E \approx 80$ GPa [12], $\nu \approx 1/3$) and $C_{0,Al} \approx 0.02$) one obtains a stress of about 450 MPa. For chromium ($\Omega_{Cr} = 1.20 \times 10^{-23}$ cm$^3$ [19], $C_{0,Cr} \approx 0.18$) a stress of

about 220 MPa can be calculated. This indicates that chromium has a much smaller effect on dislocation motion than aluminium. All other alloying elements (e.g. silicium) do not influence dislocation motion as much as aluminium and, to a smaller extent, chromium.

The transition of the deformation mechanism occurs between about 100 MPa at 750 °C and about 400 MPa at 500 °C (see Fig. 1a). It can be seen that, where dislocations escape from clouds of aluminium atoms, stress is in fair agreement with the transition to exponential creep only at the lowest temperature. The deviation between calculated and measured stress is larger at high temperatures. This is thought to be a consequence of the distribution of local stresses due to the dislocation arrangement. As shown elsewhere [12], the density of dislocations in the subgrain walls does not increase with applied stress because the misorientation angle between subgrains is independent of the applied stress. Taking the local dislocation density in the subgrain walls as the origin of high local stresses [5], it can be seen that the stresses acting on the dislocations in the subgrain walls are nearly the same for all temperatures (in the transition region). This means that in the vicinity of subgrain boundaries there will always be local stresses near the calculated breakthrough stress.

An interesting fact was shown in Reference 11. Evaluation of dislocation bowing showed that in the vicinity of subgrain boundaries the highest local effective stresses are nearly independent of the applied stress. This indicates that the drag effect of alloying elements disappears, because at higher effective stresses dislocations can escape from their dragging clouds. Dislocations which are free of Cottrell clouds can glide very fast. This produces a high dislocation intersection rate and the substructure changes from a high degree of order (subgrain walls) to a low degree (cell walls). Thus the power law breaks down.

## 5. Conclusion

It was shown that the constant structure creep exponent, $m'$, which can be obtained from stress relaxation tests as stress sensitivity of the relaxation rate at very small stress reductions, offers some advantages for the evaluation of creep behaviour.

If power-law creep is working, $m'$ is constant, while the steady-state creep exponent, $n$, which describes the stress sensitivity of steady-state creep rate, increases with applied stress. In the exponential creep region, $m'$ is linearly dependent on the applied stress. Thus the choice between these deformation mechanisms is easy.

From a combination of $m'$ with internal stress measurements, the effective stress exponent, $m$, of dislocation velocity can be calculated. If $m$ is near unity, drag-controlled dislocation motion controls deformation. This is the case in the region of power-law creep. In the exponential creep region, $m$ grows, indicating that dislocations break away from their Cottrell clouds.


## Acknowledgement

Financial support by the FWF is gratefully acknowledged (Project no. P 5574).


## References


1. S. V. RAJ, *Scripta Metall.* **20** (1986) 1333.
2. B. ILSCHNER, in "Hochtemperaturplastizität" (Springer-Verlag, Berlin, 1973).
3. O. D. SHERBY and P. M. BURKE, *Prog. Mater. Sci.* **13** (1967) 325.
4. B. REPPICH, *Z. Metallkde* **73** (1982) 697.
5. W. D. NIX and B. ILSCHNER, in "Proceedings of the 5th International Conference on the Strength of Metals and Alloys", Vol. 3, Aachen, August 1979, edited by P. Haasen, V. Gerold and G. Kostorz (Pergamon Press, Oxford, 1979) p. 1503.
6. S. TAKEUCHI and A. S. ARGON, *J. Mater. Sci.* **11** (1976) 1542.
7. A. ORLOVA and J. CADEK, *Mater. Sci. Engng* **77** (1986) 1.
8. S. U. AN, H. WOLF, S. VOGLER and W. BLUM, in "Proceedings of the 4th International Conference on Creep and Fracture of Engineering Materials and Structures", Swansea, April 1990, edited by B. Wilshire and R. W. Evans (Institute of Metals, London, 1990) 81.
9. K. TOMA, H. YOSHINAGA and S. MOROZUMI, *Trans Jpn Inst. Metals* **17** (1976) 102.
10. W. BLUM, A. ROSEN, A. CEGIELSKA and J. L. MARTIN, *Acta Metall.* **37** (1989) 2439.
11. F. GROISBÖCK and F. JEGLITSCH, *J. Mater. Sci.*, **27** (1992) 4365.
12. F. GROISBÖCK, Doctoral thesis, Leoben (1990).
13. F. GROISBÖCK and R. EBNER, *Z. Metallkde*, **82** (1991) 435.
14. M. BIBERGER and W. BLUM, *Scripta Metall.* **23** (1989) 1419.
15. F. GROISBÖCK, R. EBNER and F. JEGLITSCH, in "Proceedings of the 1st International Conference on Advanced Materials and Processing", Aachen, November 1989, edited by H. E. Exner and V. Schumacher (DGM Informationsgesellschaft, Oberursel, 1990) p. 579.
16. J. WEERTMAN, *Acta Metall.* **25** (1977) 1393.
17. W. BLUM, private communication (1990).
18. M. F. ASHBY, *Acta Metall.* **20** (1972) 887.
19. T. LYMAN (ed.), "Metals Handbook", Vol. 1, 8th Edn (American Society for Metals, Metals Park, OH, 1961).



*Received 12 April*
*and accepted 7 October 1991*